Mitochondrial outer membrane proteome of *Trypanosoma brucei* reveals novel factors required to maintain mitochondrial morphology

Moritz Niemann[1)]#, Sebastian Wiese[2)]#, Jan Mani[1)], Astrid Chanfon[1)], Christopher Jackson[3)], Chris Meisinger[1)4)], Bettina Warscheid[2)]*, André Schneider[1)]*

[1)] Department of Chemistry and Biochemistry, University of Bern, CH-3012 Bern, Switzerland

[2)] Faculty of Biology and BIOSS Centre for Biological Signalling Studies, University of Freiburg, 79104 Freiburg, Germany

[3)] Division of Human Genetics, Department of Paediatrics and Department of Clinical Research, Inselspital, University of Bern, Switzerland

[4)] Institut für Biochemie und Molekularbiologie, ZBMZ and BIOSS Centre for Biological Signalling Studies, Universität Freiburg, Freiburg, Germany

# These authors contributed equally to this work

* Corresponding authors:

André Schneider (Phone: +41 31 631 4253. Fax: +41 31 631 48 87. E-mail: andre.schneider@ibc.unibe.ch) or Bettina Warscheid (Phone: +49 761 203 2690. Fax: +49 761-203-2601. E-mail: bettina.warscheid@biologie.uni-freiburg.de)

Running title: mitochondrial OM proteome of *T. brucei*

The abbreviations used are:

OM, mitochondrial outer membrane.

ATOM, archaic translocase of the outer membrane.

VDAC, voltage-dependent anion channel.

IM, inner membrane.

POMP, present in the outer mitochondrial membrane proteome.

SUMMARY

***Trypanosoma brucei* is a unicellular parasite that causes devastating diseases in humans and animals. It diverged from most other eukaryotes very early in evolution and as a consequence has an unusual mitochondrial biology. Moreover, mitochondrial functions and morphology are highly regulated throughout the life cycle of the parasite. The outer mitochondrial membrane defines the boundary of the organelle. Its properties are therefore key for the understanding of how the cytosol and mitochondria communicate and how the organelle is integrated into the metabolism of the whole cell. We have purified the mitochondrial outer membrane of *T. brucei* and characterized its proteome using label-free quantitative mass spectrometry for protein abundance profiling in combination with statistical analysis. Our results show that the trypanosomal outer membrane proteome consists of 82 proteins, two thirds of which have never been associated with mitochondria before. 40 proteins share homology with proteins of known functions. The function of 42 proteins, 33 of which are specific for trypanosomatids, remains unknown. 11 proteins are essential for the disease-causing bloodstream form of *T. brucei* and therefore may be exploited as novel drug targets. A comparison with the outer membrane proteome of yeast defines a set of 17 common proteins that are likely present in the mitochondrial outer membrane of all eukaryotes. Known factors involved in the regulation of mitochondrial morphology are virtually absent in *T. brucei*. Interestingly, RNAi-mediated ablation of three outer membrane proteins of unknown function results in a collapse of the network-like mitochondrion of procyclic cells and for the first time identifies factors that control mitochondrial shape in *T. brucei*.**

INTRODUCTION

Trypanosomatids are unicellular parasites that cause devastating diseases in both humans and animals. They include *Trypanosoma brucei*, two subspecies of which cause human sleeping sickness, as well as *Trypanosoma cruzi* and *Leishmania* spp., which are responsible for Chagas disease and leishmaniasis, respectively. The treatment of these diseases is still in an unsatisfactory state and new drugs are urgently needed (1).

Besides their clinical importance, some trypanosomatids are highly accessible experimental model systems to investigate general biological processes. Moreover, trypanosomatids appear to have diverged from all other eukaryotes very early in evolution and therefore show many unique features, some of which may reflect primitive traits that were present in the universal ancestor of all eukaryotes (2).

Many of these features concern the mitochondrion. Its genome consists of two genetic elements, the maxi- and the minicircles, which are highly topologically interlocked and localized to a discrete region within the organelle (3). Many mitochondrial genes represent cryptogenes whose primary transcripts have to be processed by extensive RNA editing in order to become functional mRNAs (4). The mitochondrial genome lacks tRNA genes indicating that trypanosomatids, unlike most other eukaryotes, import all mitochondrial tRNAs from the cytosol (5). The mitochondrial outer membrane (OM) of trypanosomatids has an unusual protein translocase, termed ATOM (6), that shares similarity to the canonical protein import pore Tom40 (7) but also to the bacterial Omp85-like protein family that is involved in protein translocation (6,8,9).

Trypanosomatids, unlike most other eukaryotes, have a single continuous mitochondrion throughout their life and cell cycle (10,11). Its morphology changes from a complex network in procyclic cells to a single tube-like structure in the bloodstream form (12). Nothing is currently known about how the different morphologies of its mitochondrion are established and maintained.

The changes in organellar shape correlate with large functional differences between the mitochondrion of the procyclic and the bloodstream forms. Only organelles of the procyclic stage are capable of oxidative phosphorylation, whereas in the bloodstream form, energy is produced by substrate level phosphorylation (13-15).

Recently, a proteomic study of the whole *T. brucei* mitochondrion detected 401, 196 and 283 proteins that could be assigned to mitochondria with high, medium and low confidence, respectively (16). A follow up study analyzed mitochondrial membrane fractions and identified 202 proteins that contain one or more predicted transmembrane helices and that were associated with mitochondria with various levels of confidences (17). This added 65 new proteins to the previously defined mitochondrial proteome. Moreover, the proteomes of the respiratory complexes (18) and the mitochondrial ribosomes (19) have also been characterized. However, an inventory of the mitochondrial OM is still lacking. In fact, the way the mitochondria were isolated in the studies described above suggests that they are depleted for OM proteins (20).

The OM separates the organelle from the cytosol. Detailed knowledge about the OM proteome is therefore a prerequisite for a comprehensive understanding of how the cytosol and mitochondria communicate and how the organelle is integrated into the metabolism of its host cell. The OM is the first barrier imported proteins that tRNAs face while they are transported into the mitochondrion. Knowing its proteome will therefore also help to understand the molecular mechanisms of these two processes.

Presently, only four mitochondrial OM proteins are known in trypanosomatids. These are the voltage-dependent anion channel (VDAC) that serves as a metabolite transporter (21) and three components of the mitochondrial protein import system. The latter include the trypanosomal SAM50 orthologue, which mediates insertion of beta barrel proteins into the OM (22), ATOM, the general mitochondrial preprotein translocase (6) and pATOM36, which may serve as a receptor for

a subset of imported proteins (23). The situation is only marginally better outside the trypanosomatids and the only examples where global proteomic analyses of the mitochondrial OM have been performed are the two fungal species *Saccharomyces cerevisiae* (24) and *Neurospora crassa* (25) and the plant *Arabidopsis thaliana* (26). These studies detected 82 and 30 resident OM proteins, respectively, in the fungal species and 42 proteins in plants.

Here we present a comprehensive proteomic analysis of the mitochondrial OM of the procyclic form of *T. brucei*. To that end, we established a purification procedure allowing the isolation of a highly enriched OM fraction. To identify bona fide OM proteins, we employed label-free quantitative mass spectrometry to establish abundance profiles of several hundred proteins across four and six subcellular fractions including highly purified OMs. This allowed us to identify 82 proteins that could be localized to the mitochondrial OM with high confidence. Ablation of three trypanosomatid-specific proteins of unknown function affects mitochondrial morphology and thus defines the first factors controlling mitochondrial morphology in *T. brucei*. Based on a recent global RNAi study (27), 9 OM proteins are essential for normal growth under all tested conditions including the disease-causing bloodstream form of the parasite indicating that they could be novel potential drug targets.

EXPERIMENTAL PROCEDURES

Cell culture

Both procyclic wildtype *T. brucei* strain 427 and transgenic *T. brucei* strain 29-13 were used in this study. All cell lines were grown in SDM79, which was supplemented with 5% (427) or 10% (29-13) fetal calf serum (Sigma), respectively. For OM purification cells were harvested at late log phase corresponding to a density of 3.0-4.0 x 10^7 cell/ml.

Purification of the mitochondrial OM of *T. brucei*

Cells were lysed under isotonic conditions by N_2-cavitation (28). Mitochondrial vesicles were isolated by differential centrifugation and subsequent Nycodenz step gradients as described (20). Mitochondrial vesicles were used as a starting point to prepare a highly enriched mitochondrial OM fraction using a modified version of the procedure described in (29,30) (see Fig. 1A for an overview). 100 mg of mitochondrial vesicles, isolated from 4-5 x 10^{11} cells, were diluted to 10 mg/ml in swelling buffer consisting of 5 mM potassium phosphate, pH 7.2 containing 5 mM EDTA and 1 mM PMSF. The vesicles were kept under hypotonic conditions for 25 min on ice and allowed to swell. Subsequently, they were homogenized by 20 strokes using a Dounce homogenizer (Wheaton) with a loose fitting Teflon pestle to dislodge the OM from the inner membrane (IM). To separate IM vesicles and residual mitochondria from the lower density OM, the mixture was loaded on top of a 0/15/32/60% (w/v) sucrose step gradient containing buffer A (10 mM MOPS, KOH pH 7.2 and 2.5 mM EDTA). Centrifugation was done for 1 hr at 2°C with 100,000 g and both the bottom fraction (32/60% sucrose interface) corresponding to the IM as well as the top fraction (15/32% sucrose interface) corresponding to crude OM were collected. The latter was adjusted to 50% (w/v) sucrose in buffer A and overlaid with two layers consisting of an equal volume of buffer A containing 32% (w/v) sucrose and of buffer A lacking sucrose, respectively. The flotation gradient was centrifuged for 5 hrs at 2°C with 240,000 g and the fraction at the 0/32% sucrose interphase

corresponding to pure OM was collected. Approximately 300 µg OM per 100 mg mitochondrial vesicles were obtained.

Crude ER fraction was prepared using the supernatant resulting from centrifugation after the isotonic N_2-cavitation of the cells (20,28). This supernatant was subjected to a clearing spin for 30 min at 4°C with 30,000 g in order to remove remaining mitochondrial vesicles and cell debris. From this cleared supernatant the crude ER fraction was harvested by ultracentrifugation (2 hrs at 4°C with 100,000 g).

Sample preparation for proteomic analysis

Proteins from organellar fractions were precipitated using 10% trichloroacetic acid or 4:1 (v/v) methanol (MeOH)/chloroform (31). Protein pellets were obtained by centrifugation for 20 min at 4°C with 21,100 g and redissolved in 60% MeOH/20 mM NH_4HCO_3 (pH 7.8). Tryptic digestion of proteins was performed overnight at 37°C and resulting peptides were dried *in vacuo* and redissolved in 15 µl 0.1% trifluoroacetic acid (TFA).

Mass spectrometry

Ultra-high pressure LC separations were conducted on the UltiMate 3000 RSLCnano HPLC system (Thermo Scientific, Idstein, Germany). Peptides were concentrated and washed on a C18 µ-pre-column (Acclaim® PepMap µ-Precolumn Cartridge; 0.3 mm x 5 mm, particle size 5 µm, Thermo Scientific) for 10 min with 0.1% TFA at a flow rate of 30 µl/min and subsequently separated on a 25 cm x 70 µm C18-column (Acclaim PepMap RSLC column, 2 µm particle size, 100 Å pore size, Thermo Scientific, Idstein, Germany) at a flow rate of 300 nl/min with a linear gradient consisting of 4 - 26% solvent B [0.1% (v/v) FA in 84% (v/v) ACN] in 140 min and 26 - 43% solvent B in 10 min. Eluting peptides were directly analyzed by tandem mass spectrometry (MS/MS) on a LTQ-Orbitrap XL instrument (Thermo Scientific, Bremen, Germany) equipped with a nanoelectrospray

ion source. A spray voltage of 1.5 kV and an ion transfer tube temperature of 200°C were applied. The instrument was calibrated using standard compounds and operated in the data-dependent mode. Survey MS spectra from *m/z* 370 – 1700 were acquired in the orbitrap at a resolution of 60,000 at *m/z* 400 with an AGC value of 5×10^5 ions and a maximum fill time of 500 ms. A TOP5 method was applied. The five most intense multiple charged peptides were sequentially subjected to low-energy collision-induced dissociation experiments in the linear ion trap applying a target accumulation value of 10,000 with a maximum fill time of 400 ms, a normalized collision energy of 35%, an activation q of 0.25 and an activation time of 30 ms. A dynamic exclusion time of 45 s with a parent mass accuracy of 20 ppm was applied.

Data analysis

Mass spectrometric data of two independent experiments were processed separately using the software MaxQuant (version 1.2.0.18) (32,33). For protein identification, spectra were correlated with the *Trypanosoma brucei* protein database (TriTrypDB; www.tritrypdb.org; version 3.1) containing 9,826 protein entries using Andromeda (33). All searches were performed with tryptic specificity allowing up to two missed cleavages. Oxidation of methionine and acetylation of protein N-termini were considered as variable modification. No fixed modifications were considered. Raw data were recalibrated using the "first search" option of Andromeda with the full database employing a mass error of 20 ppm for precursor ions and 0.5 Da for fragment ions. Mass spectra were searched using the default settings of Andromeda. The mass tolerance for precursor and fragment ions was 6 ppm and 0.5 Da, respectively. A false discovery rate of 1% was applied on both the peptide and protein level. For retrieving information about protein abundance, the label-free protein quantification option in MaxQuant was enabled using default settings and the “match between runs”-option with a retention time window of two minutes. Only razor and unique peptides were considered for quantification. Protein intensity values were normalized to the total

ion current (TIC) of the pure mitos and the OM/ER fraction of experiment 1 and 2, respectively. To establish protein profiles, intensity values of a given protein were plotted against the different subcellular fractions and normalized to one. For statistical analysis, protein abundance profiles were hierarchically clustered using Euclidian distances and complete linkage in the R software environment. Only proteins identified and quantified in both datasets were considered for clustering analysis; mass spectra of single peptide identifications are shown in Suppl. Figure S1. For the calculation of log10 intensity plots, , intensity values were normalized to the intensity value of HSP60 (Tb927.10.6400), representing the most abundant protein in pure mitos fraction. The mean of the normalized intensity values of each protein was then calculated and multiplied with the intensity of HSP60 in experiment 2.

Proteinase K digestion

Mitochondrial vesicles (20)(25 µg each) were resuspended in 20 mM Tris, pH 7.2, 15 mM KH_2PO_4, 20 mM $MgSO_4$ and 0.6 M sorbitol in a total volume of 50 µl. Proteinase K treatment (Roche; final concentration 50 or 250 µg/ml) was done for 15 min on ice. The reactions were stopped by adding PMSF to a final concentration of 5 mM. Subsequently, mitochondrial vesicles were sedimented for 3 min at 4°C with 6,800 g in a table top centrifuge and the resulting pellet was resuspended in SDS sample buffer containing 60 mM ß-mercaptoethanol and boiled for 3 min at 95°C.

Miscellaneous

Protein concentrations were determined using the BCA protein assay reagent (Pierce). Protein samples were analyzed by conventional SDS-PAGE and immunoblotting using the Odyssey Clx infrared imaging system (Li-Cor, Biosciences). Proteins were C-terminally c-MYC-tagged; SAM35 was C-terminally tagged with the HA-epitope using a pLew100-based construct (34,35). Inducible RNAi cell lines of POMP9, 14 and 40 were prepared using pLew100-based stem-loop constructs

(35,36). As inserts, we used a 428-bp fragment (nucleotides 686-1113) of POMP9, a 360-bp fragment (nucleotides 1-360) of POMP14 and a 303-bp fragment (nucleotides 12-314) of POMP40. Immunofluoresence of paraformaldehyde fixed cells was done as described (37).

RESULTS AND DISCUSSION

Purification of the mitochondrial OM from *T. brucei*

The mitochondrial OM purification strategy for *T. brucei* was adapted according to protocols from yeast (29,30) and is outlined in Fig. 1A. In the first step, procyclic *T. brucei* cells are lysed under isotonic conditions using N_2-cavitation (28). After DNA digestion and differential centrifugation, a crude mitochondrial fraction (crude mitos) is obtained and further purified by Nycodenz gradient sedimentation yielding pure mitochondria (pure mitos), which have an intact OM (20). This fraction is subjected to a swelling step under hypotonic conditions and extensively homogenized. The aim of this step is to disrupt the OM and to dislodge it from the IM. The resulting homogenate is resolved on a sucrose gradient yielding two main fractions. The denser, more abundant one is enriched for IM markers, whereas the less dense, minor fraction corresponds to crude OM. The latter is collected and subjected to a sucrose flotation gradient again resulting in two fractions, one consisting of pure OM and the other of both ER and OM (OM/ER). Starting from 4 x 10^{11} cells, approximately 300 μg of pure OM fraction was obtained.

Selected fractions of the purification (Fig. 1A, grey boxes) were analyzed by silver staining (Fig. 1C) and on immunoblots using a panel of antisera directed against marker proteins for submitochondrial and different subcellular compartments (Fig. 1B). The results show that the previously characterized trypanosomal OM proteins, VDAC (21), SAM50 (22) and ATOM (6), are strongly enriched in the pure OM fraction. A quantification of the immunoblots indicates that the enrichment factors for the three proteins between whole cells and the pure OM fraction are between 50 to 60-fold (it should be noted that the three last lanes of the immunoblots in Fig. 1B contain 20-fold less protein than all other lanes). Markers for the intermembrane space (IMS), the IM and the matrix are strongly depleted in the pure OM fraction, indicating that there is only very little contamination with components from the other mitochondrial subcompartments. Moreover, the pure OM fraction is essentially free of cytosol, glycosomes and components of the cytoskeleton.

In the case of the ER, both BiP, a component of the ER lumen, and a tagged transmembrane subunit of the trypanosomal glycosylphospatidylinositol transamidase complex (GPI16:HA) (38) were analyzed. Both ER proteins are depleted in the pure OM fraction but to a lesser extent than the markers for the other subcellular compartments. Interestingly, the most dense fraction recovered from the sucrose flotation gradient, termed OM/ER, is enriched for the OM as well as for both ER markers.

Finally, the pure OM fraction was also subjected to electron microscopy using uranyl acetate for negative staining. This analysis revealed a population of single membrane-bounded vesicles of similar morphology but different diameters consistent with a highly enriched mitochondrial OM fraction (Suppl. Fig. S2) (39).

Mass spectrometric analysis of subcellular fractions

A eukaryotic cell contains many different membranes of which the mitochondrial OM is of minor abundance. Moreover, the OM is known to be tightly associated with the IM and to interact with parts of the ER (40). This makes it difficult, if not impossible, to prepare OM that is free of contaminants, the most likely sources of which are the IM and the ER. In order to identify bona fide OM proteins and to distinguish them from contaminants, we employed protein abundance profiling by high resolution mass spectrometry (41-43). Two independent experiments were performed to characterize the mitochondrial OM proteome. In the first, crude and pure OM fractions as well as pure mitos and OM/ER fractions were analyzed (Fig. 1A, see *). In the second experiment the analysis was extended by including the crude ER and the crude IM fraction (Fig. 1A, see °). All fractions were analyzed by high resolution LC/MS to provide a comprehensive dataset for label-free quantitative protein profiling. Table 1 provides a summary of the number of MS/MS spectra acquired as well as the number of peptides and proteins identified in individual fractions (Suppl. Tables S1A-D and S2A-D). Altogether, more than 100,000 MS/MS spectra were acquired resulting

in the identification of 2,142 unique proteins with a false discovery rate of ≤ 1%. In experiment 2, the inclusion of the crude ER and the crude IM fraction led to the identification of a further 587 proteins that were not found in experiment 1. Protein identification numbers obtained for the pure mitos and pure OM fraction from the two independent experiments were highly consistent with a variation of 4% and 11%, respectively. Moreover, the corresponding overlaps of proteins identified in these fractions were 67.6% and 59.1%, underscoring the high consistency of our data.

Localization of proteins by correlation of abundance profiles

To further distinguish between OM constituents and co-purified contaminants, we relied on quantitative feature analysis in MS survey scans using the MaxQuant algorithm (32,33). This allows to determine intensity values of all proteins identified in the four and six different subcellular fractions obtained during the two OM purifications.

Altogether, 1062 proteins were quantitatively followed through both experiments (Suppl. Table S3) and the corresponding normalized abundance profiles were calculated. Figure 2 depicts the abundance profiles of marker proteins of the mitochondrial OM (VDAC, SAM50 and ATOM) and IM (COX 4 and CYT C1) as well as the ER (BiP and GPI16). Notably, MS-based protein abundance profiles of subcellular and suborganellar marker proteins were highly reproducible between the two independent experiments (Fig. 2) and essentially congruent with the ones obtained by immunoblotting (Fig. 1B). OM proteins characteristically exhibited low intensities in crude ER, pure mitos and IM fractions, while showing a distinct maximum in pure OM fractions. Notably, the measured relative intensity of OM proteins typically increased by more than two-fold between crude and pure OM fractions, thereby facilitating the reliable identification of even minor OM constituents. Contaminants of the OM mainly derived from the ER and the IM (Fig. 1B). Such components could be well distinguished from the OM proteome based on their abundance profiles

exhibiting distinct maxima in either the crude ER or the crude IM fraction as exemplarily shown for the marker proteins GPI16, BiP and COX 4, CYT C1, respectively (Fig. 2).

Through this statistical approach, a cluster of 83 putative OM proteins was obtained. However, since it contained the inner membrane localized ADP/ATP carrier, which is the most abundant mitochondrial membrane protein and therefore the most obvious contaminant of the pure OM fraction, this protein was excluded from the cluster resulting in an OM proteome of 82 proteins (Fig. 3A, Suppl. Table S3). All cluster components are listed in Tables 2 and 3, including information about their accession number, name, predicted protein domains, molecular weight and number of putative transmembrane domains. They comprise all four previously known mitochondrial OM proteins: VDAC (21), SAM50 (22), ATOM (6) and pATOM36 (23). Using BLAST, we found 38 proteins of the OM cluster that show similarities to proteins of known function in other eukaryotes and two trypanosomatid-specific components of the OM protein import system (6,23). The function of 42 proteins (51% of the OM proteome) is unknown. These proteins were termed POMPs for present in the outer mitochondrial membrane proteome and numbered. 16 POMPs have known protein domains (Table 2) and 33 proteins (40% of the total proteome) are conserved in trypanosomatids only (Table 2, asterisks).

The power of the protein abundance profiling approach is illustrated by the fact that, except for the ADP/ATP carrier mentioned above, the OM proteome lacks all the common contaminants such as the highly abundant ribosomal proteins, eukaryotic translation elongation factor 1a and tubulins. The same applies to proteins known to reside in other submitochondrial compartments.

Interestingly MICU1 (44) the regulatory partner of the recently characterized mitochondrial Calcium uniporter MCU (45,46) was also found in the OM cluster. MICU1 is peripheral membrane protein that interacts with inner membrane protein MCU. Our results suggest the exciting possibility that MICU1 unlike assumed before might not be localized in the IM but together with MCU may form contact sites between the two mitochondrial membranes.

It should be considered in this context that our OM cluster might also contain dually localized OM proteins as long as their second localization is outside mitochondria.

Even though it was not the aim of our study, it is worth to note that our quantitative proteomics survey further allows to define a second cluster of 282 proteins that constitutes the mitochondrial IM proteome (Fig. 3A). Its components showed highest enrichment in the crude IM fraction and significant, but lower intensity values in the pure mitochondrial fraction (see Fig 2, experiment 2). Interestingly, 37% of these proteins are not found in the least stringent list of IM proteins that has been published before (17).

To demonstrate the consistency of data obtained from both experiments, the median and the middle 50% of the profiles of all the 82 and 282 proteins present in the OM and IM cluster are depicted in Figure 3B and 3C, respectively. Notably, the OM and IM proteome comprise only 4 and 13% of all the proteins identified in this study. Moreover, these constituents represent only a minor fraction of all the proteins identified in highly purified OM and crude IM fractions by high performance LC/MS (see Table 1).

In summary, the data presented here underscore the effectiveness of our quantitative proteomics strategy for gaining comprehensive and accurate information about submitochondrial proteomes.

Verification of OM localization of 7 POMPs

Despite the virtual absence of obvious contaminants, we decided to verify the localization of 7 POMPs. Protease treatment is the standard assay to establish the intramitochondrial localization of a protein and the only proteins sensitive to proteolytic cleavage in intact mitochondria are OM proteins. Transgenic cell lines were produced expressing c-MYC-tagged versions of the proteins and mitochondria were isolated under isotonic conditions, which retain the integrity of the OM (28). Isolated organelles were incubated with proteinase K, which is expected to selectively cleave OM proteins and to leave proteins of the other submitochondrial fractions intact. However, the protease

shaving assay is only informative when performed with mitochondria that have an intact OM. The intactness of the OM was assayed using immunoblots that determine the ratio of the matrix-localized heat shock protein 70 (mHSP70) to the intermembrane space protein cytochrome c (CYT C). Mitoplasts are devoid of CYT C since their OM is disrupted (Fig 4A, first lane) which results in a high mHSP70/CYT C ratio. In intact mitochondria, however, CYT C remains in the intermembrane space, yielding a much lower mHSP70/CYT C ratio. The graph in Fig. 4A shows that isolated mitochondria from all the cell lines used for the protease shaving experiments have a low mHSP70/CYT C ratio when compared to mitoplasts indicating that their OM is still intact. Fig. 4B shows that all tested POMPs can be efficiently digested by proteinase K in intact mitochondria confirming that they are bona fide mitochondrial OM proteins. The same immunoblots were also decorated with an antiserum against the IM mitochondrial carrier protein MCP-5 (47), which serves as a loading control. In addition to the 7 POMPs, we also verified the OM localization of the trypanosomal SAM35 orthologue.

Relative abundance of trypanosomal OM proteins

The OM proteome was further assessed by calculating log10 intensity plots of all proteins uniformly identified in pure mitos fractions to provide an estimate of their relative abundance. The abundance distribution of the 982 proteins, including 69 OM proteins, was found to span approximately five orders of magnitude (Fig. 5A and Suppl. Table S4). The remaining 13 putative OM proteins including also the trypanosomal SAM35 orthologue could not be detected in pure mitos fractions and are therefore not included in the intensity plots. However, based on the intensity values observed in pure OM fractions, a two orders of magnitude lower abundance of SAM35 compared with SAM50 is estimated. These findings underscore the need for effective suborganellar fractionation to detect even minor, but functionally important OM constituents. Among the four known OM proteins, SAM50 exhibits the lowest abundance, whereas VDAC represents the most

abundant OM constituent. Interestingly, ATOM was found to be a mitochondrial OM protein of high abundance, while pATOM36 (23) is approximately by a factor of 10 less abundant (Figure 5B). Among the seven new OM constituents whose localization was confirmed by protease treatment (see Fig. 4), POMP10 was found to be of similar abundance as ATOM, while POMP25 was found to be approximately three orders of magnitude less abundant than POMP10 (Fig. 5C).

The trypanosomal OM proteome contains mainly unstudied proteins

Two proteomic studies characterizing the total and the membrane proteome of the *T. brucei* mitochondrion have been published before (16,17). However, the previously detected 662 proteins that could be localized to mitochondria with high and medium confidence included only 14 proteins (17%) that are present in our OM proteome.

This is consistent with the fact that the previous proteomic analyses were performed with hypotonically isolated organelles that are depleted for the OM (20). Of all experimentally identified OM proteins, an estimated 55 have not previously been associated with the mitochondrion and to our knowledge have not been studied before.

A significant fraction of the OM proteins (30 proteins, 36.6% of the OM proteome) contains at least one predicted transmembrane helix. The relative large proportion of OM proteins that lack apparent transmembrane helices is expected since the OM purification protocol in our study does not select for integral membrane proteins but detects peripheral membrane proteins as well. Moreover, some OM proteins are beta-barrel membrane proteins, which lack classical membrane spanning domains.

Conserved features of mitochondrial OM proteomes

The mitochondrial OM proteome has been analyzed from two fungal and one plant species. In *Neurospora crassa,* 30 proteins were localized to the mitochondrial OM (estimated coverage 65%)

(25). Orthologues of virtually all of these proteins were also found in the much larger mitochondrial OM proteome of *S. cerevisiae* which consists of 82 different proteins (estimated coverage 85%) (24). In the plant *A. thaliana*, 42 proteins were assigned to the OM (estimated coverage 88%) (26). The mitochondrial OM proteome of *T. brucei* as determined in this study consists of 82 different proteins. Fungi, plants and trypanosomes belong to three different eukaryotic supergroups (48). Having defined the OM proteomes from these species therefore allows to identify a set of proteins that are likely found in the mitochondrial OM of all eukaryotes (Table 4). These universally conserved OM proteins are VDAC, Tom40, SAM50, SAM35 and the GEM1 GTPase. VDAC is the most abundant OM proteins in all species investigated and is responsible for metabolite transport across the OM. Interestingly, all systems appear to have several different VDAC isoforms. In *T. brucei,* initially only one VDAC was found (21) but more elaborate bioinformatic analysis revealed the presence of two additional highly diverged VDAC-like proteins whose functions are unknown (49). Tom40 is the general protein import channel. Also the *T. brucei* mitochondrial OM contains a protein that shows limited similarity to Tom40 (7). The protein was termed ATOM and is unique in that it shares also similarity to the bacterial Omp85-like protein family (6,8,9). SAM50 and SAM35 are components of the highly conserved beta-barrel protein insertion machinery (50). GEM1 appears to be involved in the regulation of ER/mitochondria contact sites and mitochondrial morphology, respectively (40). Its universal presence in the OM proteomes suggests that ER/mitochondria contact sites are of importance in all eukaryotes.

The sizes of the OM proteomes of unicellular *T. brucei* and *S. cerevisiae* are identical and a global comparison reveals many shared features. The fraction of OM proteins attributed to the functional groups of “lipid metabolism”, “signaling/G-proteins” and “protein folding/turnover” are of similar size in both organisms. Within the group of “lipid metabolism”, the fatty acyl CoA synthetase subunit 4, the fatty aldehyde deydrogenase and the squalene synthase are found in both OM proteomes. In the group of “signaling/G-proteins”, a number of small GTPase of the rab subfamily

are present in both the *T. brucei* and the yeast OM proteome. In the "protein folding/turnover" group, the CAAX prenyl protease is detected in both proteomes. Moreover, components of the ubiquitin protein degradation system, although not the same ones, are found in the OM of both species. All in all, we find that the orthologues of 17 different OM proteins of *T. brucei*, corresponding to 20.7% of the OM proteome, are also present in the yeast mitochondrial OM (Table 4). Except for VDAC and GEM1 as well as the components of the protein import system, the function of these conserved OM proteins is unknown.

Unique features of the OM proteome of *T. brucei*

The comparative analysis of the trypanosomal and the yeast mitochondrial OM proteomes also uncovers striking differences. Proteins categorized in the functional groups of "protein import" and "dynamics/morphology" are strongly underrepresented in the mitochondrial OM proteome of *T. brucei*, whereas the proteins associated with metabolite transport are overrepresented (Fig. 6A). The latter is mainly due to the presence of three ABC transporters that are not found in the OM proteome of yeast.

The paucity of recognizable protein import factors in the trypanosomal OM proteome is in line with the fact that even the normally conserved protein import pore of the OM (6) and a receptor-like component of the protein import system (23) are highly diverged in trypanosomes. The absence of orthologues of the other protein import factors is therefore not surprising. However, the number and the kind of proteins that need to be imported into the trypanosomatid mitochondrion are comparable to other unicellular organisms indicating that the protein import system, while different, will be of similar complexity than in other eukaryotes. We therefore expect that some of the POMPs are trypanosomatid-specific components of the mitochondrial protein import system.

The virtual absence of proteins that belong to the group "mitochondrial dynamics/morphology" in the *T. brucei* OM proteome is surprising since the main components of the mitochondrial fission and fusion machineries are conserved (51). However, it is in line with the fact that mitochondrial dynamics in trypanosomatids shows unique features.

Ablation of POMP9, 14 and 40 affects mitochondrial morphology.

The single mitochondrion of *T. brucei* divides in two only during cytokinesis to allow its transmission to the daughter cells (52,53). In trypanosomatids, mitochondrial fusion has never been observed and mitochondrial fission must be coordinated with the cell cycle. As in other systems, fission requires the dynamin-like protein, DLP1, which is the single member of the dynamin protein family found in trypanosomatids (53,54). Moreover, ablation of DLP1 in *T. brucei* caused the accumulation of cells that are blocked in cytokinesis suggesting that mitochondrial division acts as a checkpoint for cell division (53). Maintaining a single mitochondrion at all times, both the regulated fission prior to cytokinesis and the morphology change during the life cycle are expected to require as yet unknown factors associated with the trypanosomal mitochondrial OM. We therefore expect that some of the POMPs will be such factors. As a first test for this prediction, we prepared inducible RNAi cells directed against POMP9, POMP14 and POMP40. RNAi-mediated ablation shows that all three proteins are essential for normal growth in procyclic cells (data not shown). Mitochondrial morphology was analyzed by immunofluorescence microscopy using anti-ATOM antiserum (Fig. 7). Individual ablation of all three proteins dramatically altered the network-like mitochondrial structure in procyclic trypanosomes. The strongest phenotype was observed for the POMP40 RNAi cells. Their mitochondria collapsed from a highly branched structure to an essentially single straight tubule, reminiscent of the mitochondrial shape observed in the bloodstream form (55). Also for POMP9 and POMP14, induction of RNAi causes a collapse of the network. However, the phenotype is less severe and a more condensed form of the network

appears to be maintained. In conclusion, we report POMP9, POMP14 and POMP40 as being the first factors known to regulate mitochondrial morphology in *T. brucei.* These results illustrate the value of the OM proteome to identify novel factors that directly or indirectly control mitochondrial morphology.

The mitochondrial OM proteome contains essential proteins

Recently, a global high-throughput analysis was performed, which mapped the fitness costs associated with the inducible RNAi-mediated ablation of mRNAs encoded by essentially all trypanosomal ORFs (27). The effect the RNAi has on growth of *T. brucei* was measured under four different conditions: in procyclic forms after 3 days of induction, in the bloodstream forms 3 and 6 days after induction and in differentiating cells.

Nine proteins from the *T. brucei* OM proteome are essential under all tested conditions and two proteins each are essential for the bloodstream and the procyclic form, respectively. Eight OM proteins appear to be specifically required for the differentiation of the bloodstream to the procyclic form (Fig. 6B, Supp. Table S5). Preliminary validation experiments using individual RNAi cell lines against some OM proteins indicate that the global analysis is probably biased towards false negatives suggesting that the number of essential OM proteins may even be higher (data not shown).

The nine proteins that are essential under all conditions are of special interest since they are required for core essential functions. Five of them, namely ATOM, pATOM36 and POMP6, POMP14 and POMP22 are specific for trypanosomatids. The function of these three POMPs is not known, but the only essential function of mitochondrial OM proteins described so far is protein import. This suggests that these POMPs may represent as yet unknown factors of the mitochondrial protein import machinery that are specific for trypanosomatids. Moreover, the trypanosomal mitochondrion lacks tRNA genes and therefore needs to import all of its tRNAs from the cytosol (5).

Mitochondrial translation was shown to be essential not only for the procyclic but also for the bloodstream form of *T. brucei* (56) indicating that the same must be true for mitochondrial tRNA import. Thus, we expect that also the machinery for mitochondrial tRNA import is encoded by POMPs that encode core essential functions. It is even possible, as has been suggested for the mitochondrial IM (57,58), that some protein import factors may also be required for tRNA import. Interestingly, of the three newly discovered factors that are required to maintain normal mitochondrial morphology (Fig. 7), only POMP14 but not POMP9 and POMP40 are required for core essential functions as defined by (27)(Suppl. Table S5).

Concluding remarks

Trypanosoma brucei is a unicellular eukaryote that causes devastating diseases in humans and animals. It has a unique evolutionary history resulting in a mitochondrion showing many distinct features when compared to other eukaryotes. Several of these features are linked to the OM, which forms the interface between the mitochondrion and the cytosol. They include unusual protein and tRNA import systems as well as a unique mitochondrial shape that is highly regulated. The 82 OM proteins that were identified in our study will be a treasure trove to gain insight into these processes. Most of the 82 OM proteins have never been identified before and 33 are specific for trypanosomatids. The latter are of special interest since a comparison with the yeast OM proteome reveals a strong underrepresentation of protein import factors and orthologues of proteins that regulate the shape of the mitochondrion. This suggests that many of the trypanosomal OM proteins of unknown function recovered in the present study may either be required for protein import or for maintenance of mitochondrial morphology. In line with the latter prediction, we used RNAi to identify three OM proteins of unknown function as the first candidate factors for regulation of mitochondrial morphology in *T. brucei*.

Finally, it is worth noting that ATOM, pATOM36 and the three POMPs 6, 14 and 22, are essential for the bloodstream form of *T. brucei*. These proteins might therefore represent excellent novel drug targets since they are specific for trypanosomatids and essential for the disease-causing form of the parasite. Studying their function will not only be of interest for basic science but is likely to provide novel targets for future drug development.

ACKNOWLEDGEMENTS

We thank J. Bangs (University of Wisconsin-Madison), A. Jardim (McGill University), R. Jensen (John Hopkins School of Medicine), K. Matthews (University of Edinburgh), T. Seebeck (University of Bern) and F. Voncken (University of Hull) for antisera, S. Vainauskas, J. Bangs and A. Menon (Weill Cornel Medical College) for the gift of the GPI16:HA construct, and M. Schmid and A. Albisetti for their help with the proteinase K shaving experiments. M. N. gratefully acknowledges a personal fellowship of the Peter und Traudl Engelhorn foundation. Research in the groups of C. M. and B. W. were funded by the Deutsche Forschungsgemeinschaft and the Excellence Initiative of the German Federal & State Governments (EXC 294 BIOSS Centre for Biological Signalling Studies). Research in the lab of A. S. was supported by grant 138355 of the Swiss National Foundation.

REFERENCES

1. Lüscher, A., Koning, H. P. d., and Mäser, P. (2007) Chemotherapeutic strategies against *Trypanosoma brucei*: drug targets vs. drug targeting. *Curr. Pharm. Des.* **13**, 555-567
2. Cavalier-Smith, T. (2010) Kingdoms Protozoa and Chromista and the eozoan root of the eukaryotic tree. *Biol. Lett.* **6**, 342-345
3. Lukes, J., Hashimi, H., and Zíková, A. (2005) Unexplained complexity of the mitochondrial genome and transcriptome in kinetoplastid flagellates. *Curr. Genet.* **48**, 277-299
4. Stuart, K. D., Schnaufer, A., Ernst, N. L., and Panigrahi, A. K. (2005) Complex management: RNA editing in trypanosomes. *Trends Biochem. Sci.* **30**, 97-105
5. Schneider, A. (2011) Mitochondrial tRNA Import and Its Consequences for Mitochondrial Translation. *Ann. Rev. Biochem.* **80**, 1033-1053
6. Pusnik, M., Schmidt, O., Perry, A. J., Oeljeklaus, S., Niemann, M., Warscheid, B., Lithgow, T., Meisinger, C., and Schneider, A. (2011) Mitochondrial preprotein translocase of trypanosomatids has a bacterial origin. *Curr. Biol.* **21**, 1738-1743
7. Zarsky, V., Tachezy, J., and Dolezal, P. (2012) Tom40 is likely common to all mitochondria. *Curr Biol.* **22**, R479-R481
8. Pusnik, M., Schmidt, O., Perry, A. J., Oeljeklaus, S., Niemann, M., Warscheid, B., Meisinger, C., Lithgow, T., and Schneider, A. (2012) Response to Zarsky et al. *Curr. Biol.* **22**, R481-R482
9. Harsman, A., Niemann, M., Pusnik, M., Schmidt, O., Burmann, B. M., Hiller, S., Meisinger, C., Schneider, A., and Wagner, R. (2012) Bacterial origin of a mitochondrial outer membrane protein translocase: New perspectives from comparative single channel electrophysiology. *J. Biol. Chem.* **287**, 31437-31445
10. Simpson, L., and Kretzer, F. (1997) The mitochondrion in dividing *Leishmania tarentolae* cells is symmetric and circular and becomes a single asymmetric tubule in non-dividing cells due to division of the kinetoplast portion. *Mol. Biochem. Parasitol.* **87**, 71-78
11. Tyler, K. M., Matthews, K. R., and Gull, K. (1997) The bloodstream differentiation-division of Tryranosoma brucei studied using mitochondrial markers. *Proc. R. Soc. Lond.* **264**, 1481-1490

12. Matthews, K. R. (2005) The developmental cell biology of Trypanosoma brucei. *J. Cell Sci.* **118**, 283-290
13. Priest, J. W., and Hajduk, S. L. (1994) Developmental regulation of mitochondrial biogenesis in *Trypanosoma brucei*. *J. Bioenerget. Biomemb.* **26**, 179-191
14. Schneider, A. (2001) Unique aspects of mitochondrial biogenesis in trypanosomatids. *Int. J. Parasitol.* **31**, 1403-1415
15. Besteiro, S., Barrett, M. P., Riviere, L., and Bringaud, F. (2005) Energy generation in insect stages of *Trypanosoma brucei*: metabolism in flux. *Trends Parasitol.* **21**, 185-191
16. Panigrahi, A. K., Ogata, Y., Zíková, A., Anupama, A., Dalley, R. A., Acestor, N., Myler, P. J., and Stuart, K. D. (2009) A comprehensive analysis of Trypanosoma brucei mitochondrial proteome. *Proteomics* **9**, 434-450
17. Acestor, N., Panigrahi, A. K., Ogata, Y., Anupama, A., and Stuart, K. D. (2009) Protein composition of *Trypanosoma brucei* mitochondrial membranes. *Proteomics* **9**, 5497-5508
18. Acestor, N., Zíková, A., Dalley, R. A., Anupama, A., Panigrahi, A. K., and Stuart, K. D. (2011) *Trypanosoma brucei* mitochondrial respiratome: composition and organization in procyclic form. *Mol. Cell. Proteomics*, doi: 10.1074/mcp.M1110.006908
19. Zíková, A., Panigrahi, A. K., Dalley, R. A., Acestor, N., Anupama, A., Ogata, Y., Myler, P. J., and Stuart, K. (2008) Trypanosoma brucei mitochondrial ribosomes: affinity purification and component identification by mass spectrometry. *Mol. Cell. Proteomics* **7**, 1286-1296
20. Schneider, A., Charrière, F., Pusnik, M., and Horn, E. K. (2007) Isolation of mitochondria from procyclic *Trypanosoma brucei*. *Methods Mol. Biol.* **372**, 67-80
21. Pusnik, M., Charrière, F., Mäser, P., Waller, R. F., Dagley, M. J., Lithgow, T., and Schneider, A. (2009) The single mitochondrial porin of *Trypanosoma brucei* is the main metabolite transporter in the outer mitochondrial membrane. *Mol. Biol. Evol.* **26**, 671-680
22. Sharma, S., Singha, U. K., and Chaudhuri, M. (2010) Role of Tob55 on mitochondrial protein biogenesis in Trypanosoma brucei. *Mol. Biochem. Parasitol.* **174**, 89-100
23. Pusnik, M., Mani, J., Schmid, O., Niemann, M., Oeljeklaus, S., Schnarwiler, F., Warscheid, B., Lithgow, T., Meisinger, C., and Schneider, A. (2012) An essential novel component of the non-canonical mitochondrial outer membrane protein import system of trypanosomatids. *Mol. Biol. Cell* 23, 3420-3428
24. Zahedi, R. P., Sickmann, A., Boehm, A. M., Winkler, C., Zufall, N., Schönfisch, B., Guiard, B., Pfanner, N., and Meisinger, C. (2006) Proteomic analysis of the yeast

mitochondrial outer membrane reveals accumulation of a subclass of preproteins. *Mol. Biol. Cell.* **17**, 1436-1450

25. Schmitt, S., Prokisch, H., Schlunck, T., Camp, D. G., Ahting, U., Waizenegger, T., Scharfe, C., Meitinger, T., Imhof, A., Neupert, W., Oefner, P. J., and Rapaport, D. (2006) Proteome analysis of mitochondrial outer membrane from Neurospora crassa. *Proteomics* **6**, 72-80
26. Duncan, O., Taylor, N. L., Carrie, C., Eubel, H., Kubiszewski-Jakubiak, S., Zhang, B., Narsai, R., Millar, A. H., and Whelan, J. (2011) Multiple lines of evidence localize signaling, morphology, and lipid biosynthesis machinery to the mitochondrial outer membrane of Arabidopsis. *Plant Physiol.* **157**, 1093-1113
27. Alsford, S., Turner, D. J., Obado, S. O., Sanchez-Flores, A., Glover, L., Berriman, M., Hertz-Fowler, C., and Horn, D. (2011) High-throughput phenotyping using parallel sequencing of RNA interference targets in the African trypanosome. *Genome Res.* **21**, 915-924
28. Hauser, R., Pypaert, M., Häusler, T., Horn, E. K., and Schneider, A. (1996) In vitro import of proteins into mitochondria of *Trypanosoma brucei* and *Leishmania tarentolae*. *J. Cell Sci.* **109**, 517-523
29. Alconada, A., Gärtner, F., Hönlinger, A., Kübrich, M., and Pfanner, N. (1995) Mitochondrial receptor complex from *Neurospora crassa* and *Saccharomyces cerevisiae*. *Methods Enzymol.* **260**, 263-286
30. Mayer, A., Driessen, A., Neupert, W., and Lill, R. (1995) Purified and protein-loaded mitochondrial outer membrane vesicles for functional analysis of preprotein transport. *Methods Enzymol.* **260**, 252-263
31. Wessel, D., and Fugge, U. I. (1984) A method for the quantitative recovery of protein in dilute solution in the presence of detergents and lipids. *Anal. Biochem.* **138**, 141-143
32. Cox, J., and Mann, M. (2008) MaxQuant enables high peptide identification rates, individualized p.p.b.-range mass accuracies and proteome-wide protein quantification. *Nat. Biotechnol.* **26**, 1367–1372
33. Cox, J., Neuhauser, N., Michalski, A., Scheltema, R. A., Olsen, J. V., and Mann, M. (2011) Andromeda: A Peptide Search Engine Integrated into the MaxQuant Environment. *J. Proteome Res.* **10**, 1794-1805
34. Oberholzer, M., Morand, S., Kunz, S., and Seebeck, T. (2005) A vector series for rapid PCR-mediated C-terminal in situ tagging of *Trypanosoma brucei* genes. *Mol. Biochem. Parasitol.* **145**, 117-120

35. Wirtz, E., Leal, S., Ochatt, C., and Cross, G. A. (1999) A tightly regulated inducible expression system for conditional gene knock-outs and dominant-negative genetics in *Trypanosoma brucei*. *Mol. Biochem. Parasitol.* **99**, 89-101

36. Bochud-Allemann, N., and Schneider, A. (2002) Mitochondrial substrate level phosphorylation is essential for growth of procyclic *Trypanosoma brucei*. *J. Biol. Chem.* **277**, 32849-32854

37. Sherwin, T., Schneider, A., Sasse, R., Seebeck, T., and Gull, K. (1987) Distinct localization and cell cycle dependence of COOH terminally tyrosinolated a-tubulin in the microtubules of *Trypanosoma brucei* brucei. *J. Cell Biol.* **104**, 439-445

38. Smith, T. K., and Butikofer, P. (2010) Lipid metabolism in *Trypanosoma brucei*. *Mol. Biochem. Parasitol.* **172**, 66-79

39. Parsons, D. F., Williams, G. R., and Chance, B. (1966) Characteristics of isolated and purified preparations of the outer and inner membranes of mitochondria. *Ann. NY Acad. Sci.* **137**, 643-666

40. Michel, A. H., and Kornmann, B. (2012) The ERMES complex and ER-mitochondria connections. *Biochem. Soc. Trans.* **40**, 445-450

41. Andersen, J. S., Christopher, J., Wilkinson, J., Mayor, T., Mortensen, P., Nigg, E. A., and Mann, M. (2003) Proteomic characterization of the human centrosome by protein correlation profiling. *Nature* **426**, 570-574

42. Foster, L. J., Hoog, C. L. d., Zhang, Y., Zhang, Y., Xie, X., Moohta, V. K., and Mann, M. (2006) A mammalian organelle map by protein correlation profiling. *Cell* **125**, 187-199

43. Wiese, S., Gronemeyer, T., Ofman, R., Kunze‖, M., Grou, C. P., Almeida, J. A., Eisenacher, M., Stephan, C., Hayen, H., Schollenberger, L., Korosec, T., Waterham, H. R., Schliebs, W., Erdmann, R., Berger, J., Meyer, H. E., Just, W., Azevedo, J. E., Wanders, R. J. A., and Warscheid, B. (2007) Proteomics characterization of mouse kidney peroxisomes by tandem mass spectrometry and protein correlation profiling. *Mol. Cell. Proteomics* **6**, 2045-2057

44. Perocchi, F., Gohil, V. M., Girgis, H. S., Bao, X. R., McCombs, J. E., Palmer, A. E., and Mootha, V. K. (2010) MICU1 encodes a mitochondrial EF hand protein required for Ca2+ uptake. *Nature* **467**, 291-296

45. Stefani, D. D., Raffaello, A., Teardo, E., Szabò, I., and Rizzuto, R. (2011) A forty-kilodalton protein of the inner membrane is the mitochondrial calcium uniporter. *Nature* **476**, 336-340

46. Baughman, J. M., Perocchi, F., Girgis, H. S., Plovanich, M., Belcher-Timme, C. A., Sancak, Y., Bao, X. R., Strittmatter, L., Goldberger, O., Bogorad, R. L., Koteliansky, V., and Mootha, V. K. (2011) Integrative genomics identifies MCU as an essential component of the mitochondrial calcium uniporter. *Nature* **476**, 341-345

47. Colasante, C., Diaz, P. P., Clayton, C., and Voncken, F. (2009) Mitochondrial carrier family inventory of *Trypanosoma brucei brucei*: Identification, expression and subcellular localisation. *Mol. Biochem. Parasitol.* **167**, 104-117

48. Dacks, J. B., Walker, G., and Field, M. C. (2008) Implications of the new eukaryotic systematics for parasitologists. *Parasitol. Int.* **57**, 97-104

49. Flinner, N., Schleiff, E., and Mirus, O. (2012) Identification of two voltage-dependent anion channel-like protein sequences conserved in Kinetoplastida. *Biol. Lett.* **8**, 446-449

50. Schmidt, O., Pfanner, N., and Meisinger, C. (2010) Mitochondrial protein import: from proteomics to functional mechanisms. *Nat. Rev. Mol. Cell. Biol.* **11**, 655-667

51. Westermann, B. (2010) Mitochondrial fusion and fission in cell life and death. *Nat. Rev. Mol. Cell. Biol.* **11**, 872-884.

52. Crausaz-Esseiva, A., Chanez, A.-L., Bochud-Allemann, N., Martinou, J. C., Hemphill, A., and Schneider, A. (2004) Temporal dissection of Bax-induced events leading to fission of the single mitochondrion in *Trypanosoma brucei*. *EMBO Rep.* **5**, 268-273

53. Chanez, A.-L., Hehl, A., Engstler, M., and Schneider, A. (2006) Ablation of the single dynamin of *T. brucei* blocks mitochondrial fission and endocytosis and leads to a precise cytokinesis arrest. *J. Cell Sci.* **119**, 2968-2974

54. Morgan, G. W., Goulding, D., and Field, M. C. (2004) The single dynamin-like protein of *Trypanosoma brucei* regulates mitochondrial division and is not required for endocytosis. *J. Biol. Chem.* **279**, 10692-10701

55. Vassella, E., Straesser, K., and Boshart, M. (1997) A mitochondrion-specific dye for multicolour fluorescent imaging of Trypanosoma brucei. *Mol. and Bioch. Parasitol.* **90**, 381-385

56. Cristodero, M., Seebeck, T., and Schneider, A. (2010) Mitochondrial translation is essential in bloodstream forms of Trypanosoma brucei. *Mol. Microbiol.* **78**, 757-769

57. Tschopp, F., Charrière, F., and Schneider, A. (2011) In vivo study in Trypanosoma brucei links mitochondrial transfer RNA import to mitochondrial protein import. *EMBO Rep.* **12**, 825-832

58. Seidman, D., Johnson, D., Gerbasi, V., Golden, D., Orlando, R., and Hajduk, S. (2012) Mitochondrial membrane complex that contains proteins necessary for tRNA import in *Trypanosoma brucei*. *J. Biol. Chem.* **287**, 8892-8903

FIGURE LEGENDS

Figure 1. Purification of mitochondrial OM of *T. brucei*. *A*, Outline of the OM purification scheme. The fractions that were analyzed in the immunoblot in *B* are highlighted by grey boxes. The fractions of the first and second independent OM purification that were analyzed by mass spectrometry are marked by * and °, respectively. *B*, 20 μg and 1 μg of the indicated fractions were analyzed on immunoblots using antisera directed against the indicated marker proteins of the subcellular compartments depicted on the left. Antisera directed against the following proteins were used: COX 4, cytochrome oxidase subunit 4; CYT C1, cytochrome C1; P0, ribosomal stalk protein P0; PEX14, glycosomal membrane protein PEX14; αTUB, α-tubulin; PFR, paraflagellar rod proteins; BiP, ER-localized Hsp70-like chaperone. The broken line indicates that a lane was removed electronically between the "crude OM" and the "pure OM" fractions. *C*, Silver stain of a gel containing the same fractions as were analyzed on the immunoblot in *B*.

Figure 2. Abundance profiles of marker proteins. The intensities of selected marker proteins of the OM (VDAC, SAM50, ATOM), the IM (COX 4, CYT C1) and the ER (BiP, GPI16) were measured by label-free quantitative mass spectrometry, normalized and plotted against the corresponding subcellular fractions obtained during OM preparations in experiment 1 and 2. COX 4, cytochrome oxidase subunit 4; CYT C1, cytochrome C1; BiP, ER-localized Hsp70-like chaperone.

Figure 3. Defining the mitochondrial OM proteome by protein profiling and cluster analysis. *A*, 1062 proteins were quantitatively followed through four and six distinct subcellular fractions obtained during the purification of OMs in experiment 1 and 2, respectively. Abundance profiles of proteins were calculated and subjected to hierarchical clustering allowing to define a cluster of putative OM (black bar) and IM (dark grey bar) proteins. *B* and *C,* Normalized average abundance

profiles of all proteins of the OM and IM cluster. The median (black line) and the middle 50% (shaded area) are indicated.

Figure 4. Validation of the localization of selected OM proteins by protease treatment of intact mitochondria. *A*, Upper panel, 10 μg each of hypotonically isolated mitoplasts from wild-type cells and isotonically isolated mitochondria (20) containing the indicated c-MYC-tagged proteins were analyzed by immunoblots using antibodies directed against mHSP70 and CYT C, respectively. Graph below, quantification of the mHSP70/CYT C ratio for the samples shown above. *B*, The same mitochondria (25 μg each) that are shown in *A* were left untreated or incubated with proteinase K for 15 min on ice. POMP14, 16, 25, 39, 40 and SAM35 were treated with 50 μg/ml of proteinase K, whereas POMP9 and 10 received 250 μg/ml of proteinase K. Subsequently, samples were analyzed by immunoblotting using antisera directed against the c-MYC and HA epitopes. Antibodies directed against the IM protein MCP-5 were used as a loading control.

Figure 5. Abundance of trypanosomal OM proteins. Log10 intensity plots were calculated based on normalized intensity values of proteins identified in pure mitos fractions of experiment 1 and 2. The relative abundance of 982 proteins is shown. OM proteins are marked by a rhombus. *A*, The abundance distribution of 69 OM proteins identified in pure mitos fractions covers nearly four orders of magnitude. *B*, The relative abundance levels of the four known OM proteins are shown. VDAC is the most abundant OM protein, whereas SAM50 is approximately 100-times less abundant than VDAC. C, Abundance distribution of all seven validated POMPs.

Figure 6. Comparison of the OM proteomes of *T. brucei* and *S. cerevisiae* according to functional groups. *A*, Histograms depicting the number of trypanosomal and yeast mitochondrial OM proteins that were classified into the functional groups indicated in Table 2 and 3. *B*, Histogram

depicting the number of mitochondrial OM proteins of *T. brucei* that according to the global RNAi analysis of Alsford et al. (27) are essential (i) for growth under all tested conditions (0-0-0-0), (ii) for growth of either bloodstream (0-0-1-0) or procyclic forms (1-1-0-0) only, or (iii) for differentiation of bloodstream to procyclic forms only (1-1-1-0). The binary code in parentheses is described in (27). For details see Supp. Table S5.

Figure 7. Ablation of POMP9, 14 and 40 affects mitochondrial morphology. Procyclic 29-13 cell lines allowing tetracycline inducible ablation of POMP9, POMP14 and POMP40 were tested for alterations of mitochondrial morphology. Left panels, uninduced (-tet) and induced (+tet) cells were stained for DNA using 4′-6-diamidino-phenylindole (DAPI) (blue). The outlines of the cells have been traced in the phase contrast channel and are projected onto the stained pictures. The mitochondrion from uninduced (-tet) and induced (+tet) RNAi cell lines was visualized using anti-ATOM antiserum (green). The percentage of induced cells showing an altered mitochondrial morphology was 96%, 96% and 98% for POMP9, POMP14 and POMP40, respectively. Scale corresponds to 10 μm.

Table 1. Overview of MS/MS data and protein identification numbers obtained by proteomic analysis of distinct subcellular fractions from two independent OM purification experiments.

		Experiment 1					Experiment 2						
	total (1 + 2)	**total**	**pure mitos**	**crude OM**	**pure OM**	**OM /ER**	**total**	**crude ER**	**pure mitos**	**crude IM**	**crude OM**	**pure OM**	**OM /ER**
MS/MS spectra	117,450	36,035	11,547	8,331	8,304	7,853	81,415	13,054	14,238	13,045	13,751	11,768	15,558
Identified spectra	45,013	14,430	6,128	2,932	2,691	2,679	30,583	4,761	5,467	4,828	5,042	4,132	6,353
Identified proteins	2,142	1,309	1,094	711	609	689	1,896	1,169	1,046	1,006	984	688	1,122

Table 2. High confidence *T. brucei* mitochondrial OM proteins of unknown functions.

Accession number	Name	Predicted domains	MW	TMD
Tb09.160.1070	POMP1		41.5	1
Tb09.160.1310*	POMP2		66.5	1
Tb09.160.1330	POMP3		41.2	2
Tb09.160.4440	POMP4		30.5	--
Tb09.211.0760*	POMP5		28.7	--
Tb09.211.1940*	POMP6		19	--
Tb09.211.3500*	POMP7		58.2	--
Tb09.211.3990*	POMP8		27.9	4
Tb11.01.3290*	POMP9	TPR, HCP repeats	69	--
Tb11.01.4740*	POMP10		62.2	1
Tb11.02.0180*	POMP11		41.6	6
Tb11.02.0350*	POMP12		53	--
Tb11.02.0600*	POMP13	WD40 repeat-like	39.6	1
Tb11.02.3310*	POMP14		13.6	--
Tb11.02.5105*	POMP15		15	--
Tb11.02.5660*	POMP16	armadillo-type fold	46.2	1
Tb11.52.0006	POMP17	prefoldin and myosin superfamily	139	--
Tb927.1.3800*	POMP18	OsmC-like	19.9	--
Tb927.10.510*	POMP19		37.1	--
Tb927.10.9140*	POMP20	FAD/nucleotide binding	71.9	--
Tb927.10.11030*	POMP21		11.3	--
Tb927.2.5530*, Tb927.2.5610*	POMP22		162.5	--
Tb927.3.1080*	POMP23	DUF1295	28.4	4
Tb927.3.3130*	POMP24		178.1	1
Tb927.3.3520*	POMP25	SAM motif	47.6	--
Tb927.3.4640*	POMP26	DUF125	30.4	4
Tb927.4.1540	POMP27		55.2	1
Tb927.4.1590*	POMP28		39.7	--
Tb927.4.1670	POMP29	cytochrome b5-like, heme-binding	17.4	--
Tb927.6.1550	POMP30	LRR (RNI-like superfamily)	38.9	1
Tb927.6.3680*	POMP31		27.9	3
Tb927.6.4180	POMP32	FUN	16.3	2
Tb927.7.2960*	POMP33	Ca-binding EF-hand	51.6	--
Tb927.7.4890*	POMP34		92.7	1
Tb927.7.4980*	POMP35	Zn-finger	43.4	1
Tb927.7.5470*	POMP36	Ca-binding EF-hand	74.7	1
Tb927.7.7210*	POMP37	CHP	77.5	--
Tb927.8.1470*	POMP38		62.3	--
Tb927.8.2070*, Tb927.8.2260*, Tb927.8.2270*, Tb927.8.2280*	POMP39		21.8	-- --
Tb927.8.4380*	POMP40		11.9	1
Tb927.8.5130*	POMP41		62.3	--
Tb927.8.6080	POMP42		38.1	--

* conserved in trypanosomatids only

Table 3. High confidence *T. brucei* mitochondrial OM proteins sorted according to functional groups.

Accession number	Name/Description	MW	TMD
Transport (ions and metabolites)			
Tb11.01.2550	VDAC-like	30.9	--
Tb11.03.0540	ABC transporter, putative	76.3	6
Tb927.1.4420	ABC transporter, putative	104.7	--
Tb927.2.2510, Tb927.2.2520	VDAC	29.2	--
Tb927.2.5410	ABC-transporter, putative; multidrug resistance protein	142.7	1
Tb927.4.1610	VDAC-like	39.6	--
Tb927.8.1850	MICU1, mitochondrial Calcium-uptake 1	45.7	--
Transport (protein)			
Tb09.211.1240	ATOM	38.3	--
Tb927.3.4380	SAM50	53.6	--
Tb927.7.5700	pATOM36	36	--
Tb927.8.6600	SAM35, putative	35.6	--
Signaling/G-proteins			
Tb09.211.2330	small GTPase/GTP-binding protein, putative	23.8	--
Tb11.01.5660	cyclin 2,G1 cyclin	24.3	--
Tb11.01.6890	small GTPase/ras-related protein rab-2a, putative	23.5	--
Tb927.10.1070	cell division protein kinase 2 homolog 1	39.6	--
Tb927.7.7170	CYC2-like cyclin, putative	79	--
Tb927.8.560	GEM1, putative	64.6	1
Tb927.8.4610	small GTP binding protein Rab1 (Trab1)	24	--
Lipid metabolism			
Tb09.160.2770	fatty acyl CoA synthetase 1	79	--
Tb09.160.2840	fatty acyl CoA synthetase 4	77.9	--
Tb09.211.4600	short-chain dehydrogenase, putative	51.1	--
Tb11.01.1780	short-chain dehydrogenase, putative	34	2
Tb927.3.1840	3-oxo-5-alpha-steroid 4-dehydrogenase, putative	33.4	4
Tb927.6.3050	fatty aldehyde dehydrogenase family, putative	59.7	--
Tb927.6.3630	sphingosine 1-phosphate lyase, putative	59.5	--
Tb927.6.710	dephospho-CoA kinase, putative	26.9	1
Tb927.8.7120	squalene synthase, putative	51.5	--
Protein folding/turnover			
Tb09.211.0680	CAAX prenyl protease 1, putative	48.9	5
Tb11.01.4060	ubiquitin carboxyl-terminal hydrolase, putative	89.1	--
Tb927.7.540	chaperone protein DNAj, putative	50.7	--
Tb927.7.990	chaperone protein DNAj, putative	86.6	--
Redox enzymes			
Tb09.211.4110	NADPH-cytochrome p450 reductase, putative	76.9	1
Tb11.01.1690	NIDM subunit of complex I	30.3	--
Tb11.01.5225	cytochrome b5, putative	12.9	1
Tb927.2.5180	aldo-keto reductase, putative	38.3	--
Morphology			
Tb927.5.960	MSP-1, putative	37.2	--
Other/rest			
Tb09.160.4560	arginine kinase	44.7	--
Tb927.5.2380	hydrolase, alpha/beta fold family, putative	34.4	--
Tb927.6.2540	DREV methyltransferase, putative	35.9	--
Tb927.6.3510	tRNA modification enzyme, putative	59.7	1

Table 4. Comparison of mitochondrial OM proteomes from *T. brucei, S. cerevisiae* and *A. thaliana*.

Protein	***T. brucei***	***S. cerevisiae***	***A. thaliana***
VDAC, VDAC-like proteins	3	2	4
SAM50	1	1	2
SAM35	1	1	1
TOM40[1]	(1)	1	1
GEM1 (Miro GTPase)	1	1	1
Small GTPase/GTP binding protein/G-protein, rab subfamily[2]	3	5	--
Fatty acyl CoA synthetase 4	1	1	--
Fatty aldehyde dehydrogenase	1	1	--
CAAX prenyl protease 1 (metallo-peptidase)	1	1	--
MSP-1	1	1	--
Hypothetical protein, conserved — FUN domain	1	1	--
Squalene synthase	1	1	--
NADPH-cytochrome p450 reductase	1	1	--
NADH-cytochrome b5 reductase	--	1	1
Aminoacyl-tRNA hydrolase	--	1	1

[1] ATOM of *T. brucei* has similarity to both the bacterial Omp85-like protein family and to eukaryotic Tom40.

[2] The putative small GTPases identified in *T. brucei* all belong to the rab subfamily but cannot be categorized further with adequate levels of confidence.

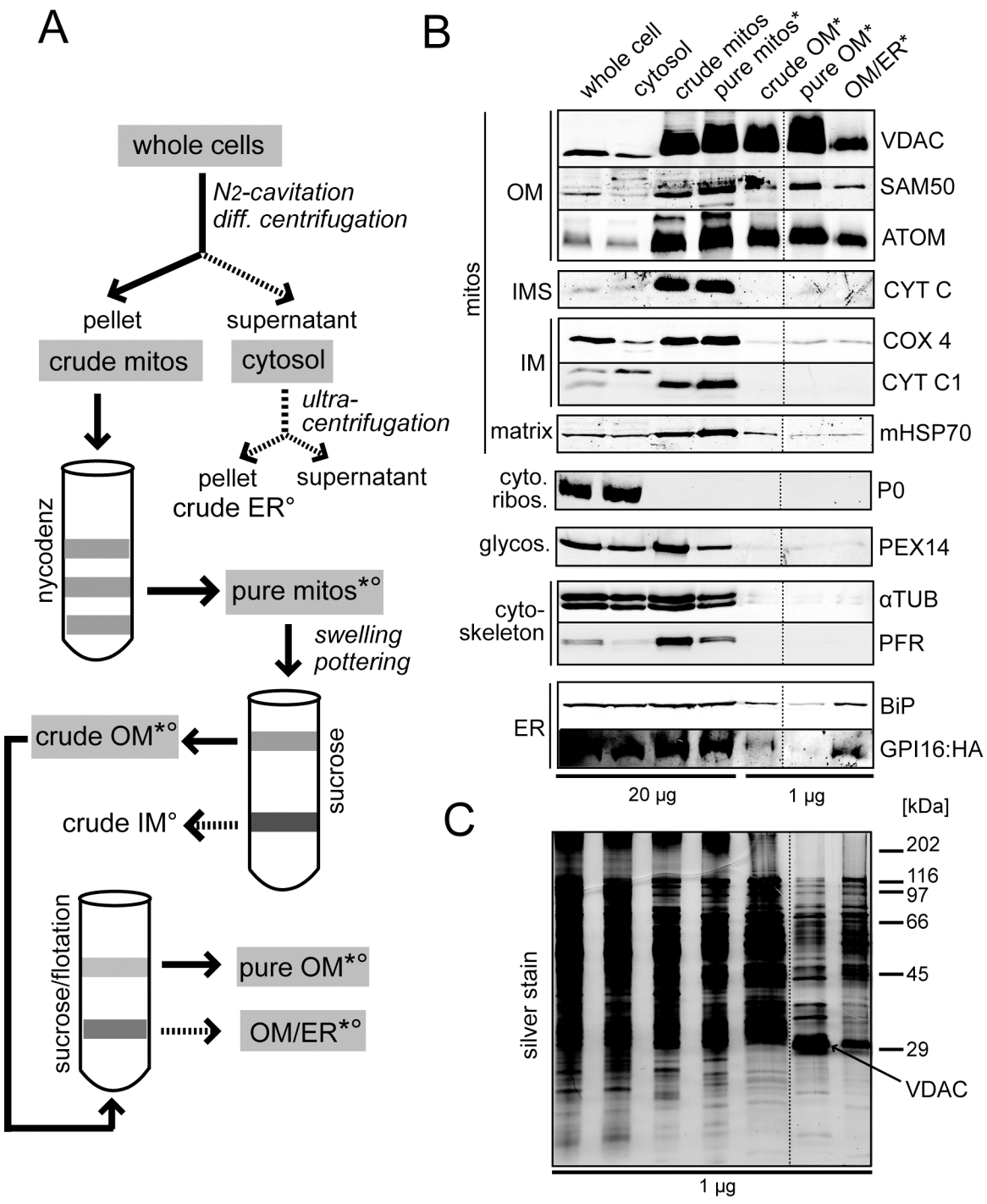
A
whole cells
N2-cavitation
diff. centrifugation
pellet
supernatant
crude mitos
cytosol
ultra-
centrifugation
pellet
supernatant
crude ER°
nycodenz
pure mitos*°
swelling
pottering
crude OM*°
crude IM°
sucrose
sucrose/flotation
pure OM*°
OM/ER*°
B
whole cell
cytosol
crude mitos
pure mitos*
crude OM*
pure OM*
OM/ER*
mitos
OM
IMS
IM
matrix
VDAC
SAM50
ATOM
CYT C
COX 4
CYT C1
mHSP70
cyto.
ribos.
P0
glycos.
PEX14
cyto-
skeleton
αTUB
PFR
ER
BiP
GPI16:HA
20 µg
1 µg
C
[kDa]
202
116
97
66
45
29
VDAC
silver stain
1 µg

Figure 1

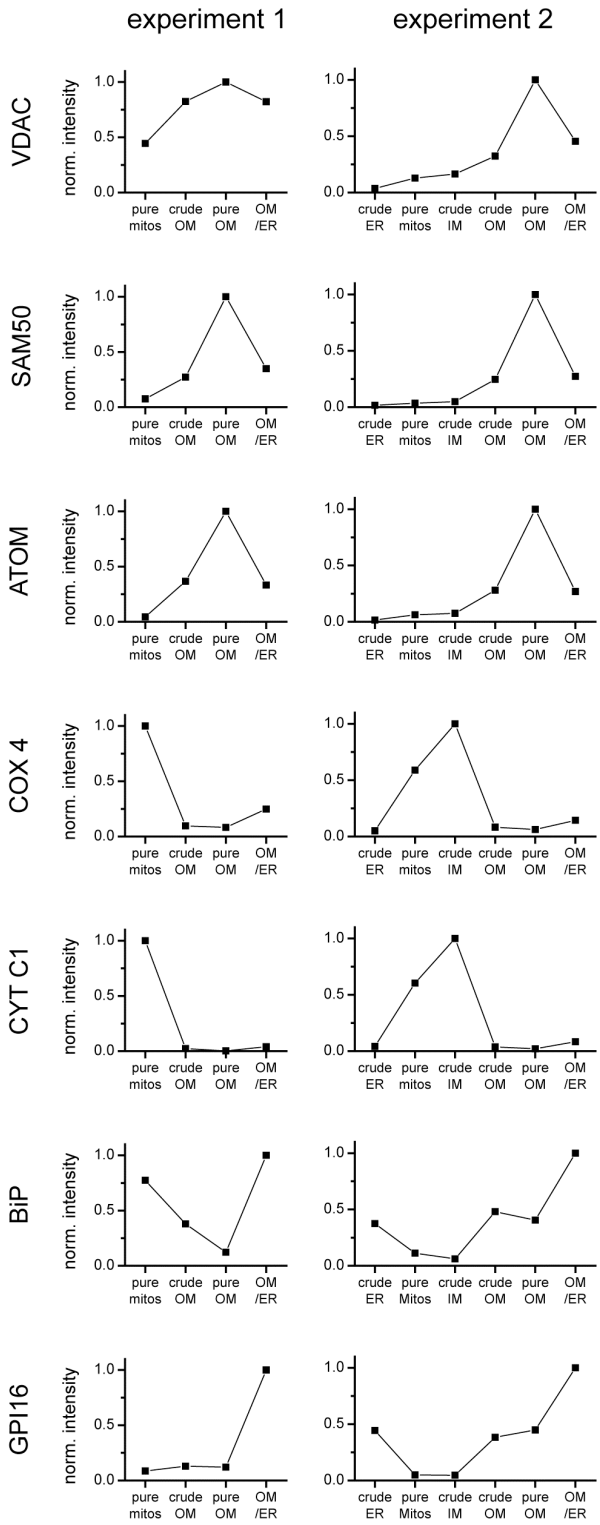
experiment 1
experiment 2
VDAC
SAM50
ATOM
COX 4
CYT C1
BiP
GPI16
norm. intensity
1.0
0.5
0.0
pure mitos
crude OM
pure OM
OM /ER
crude ER
pure mitos
crude IM
crude OM
pure OM
OM /ER
pure Mitos

Figure 2

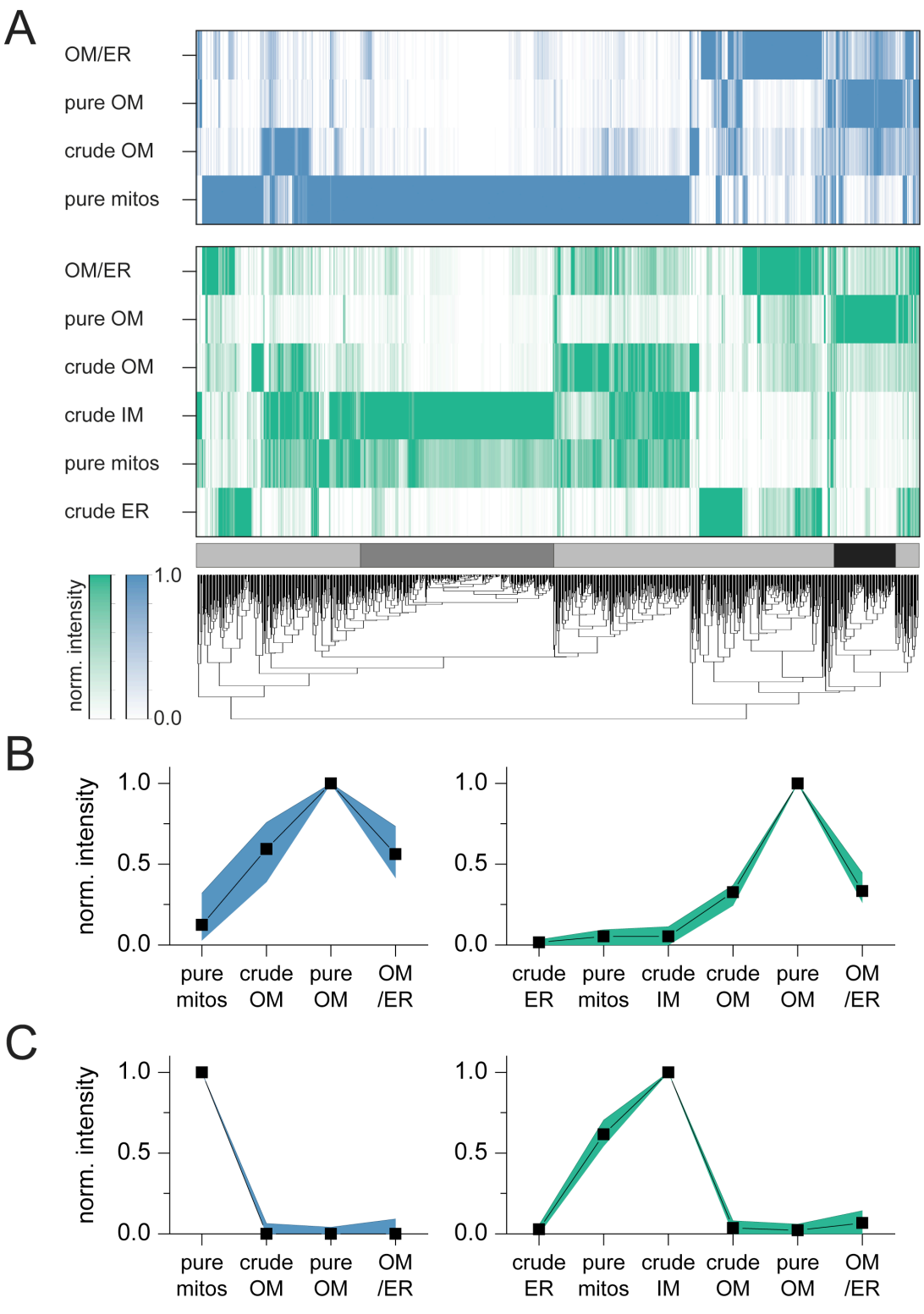
A
OM/ER
pure OM
crude OM
pure mitos
OM/ER
pure OM
crude OM
crude IM
pure mitos
crude ER
norm. intensity
1.0
0.0
B
norm. intensity
1.0
0.5
0.0
pure mitos
crude OM
pure OM
OM /ER
crude ER
pure mitos
crude IM
crude OM
pure OM
OM /ER
C
norm. intensity
1.0
0.5
0.0
pure mitos
crude OM
pure OM
OM /ER
crude ER
pure mitos
crude IM
crude OM
pure OM
OM /ER

Figure 3

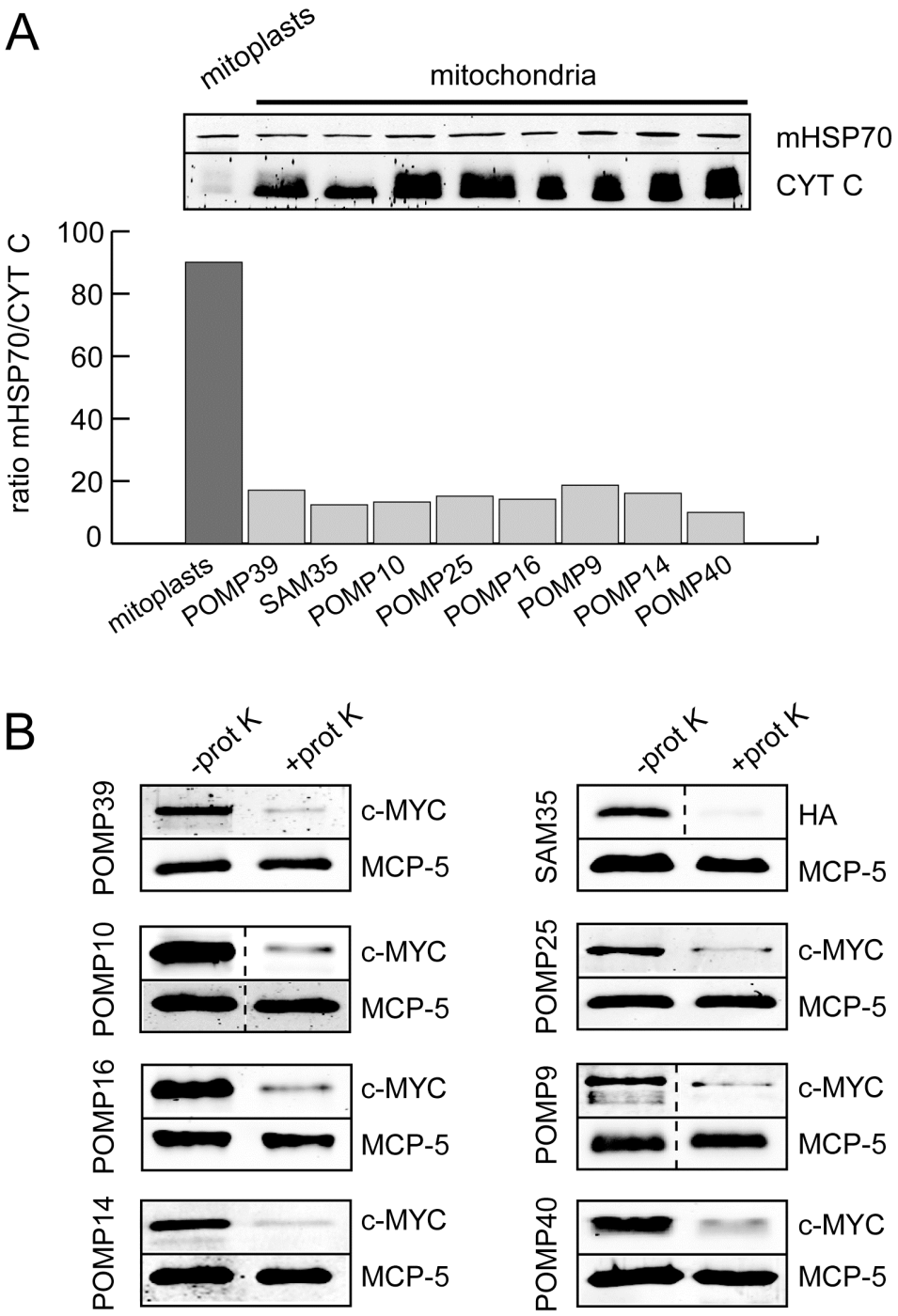
A
mitoplasts
mitochondria
mHSP70
CYT C
ratio mHSP70/CYT C
100
80
60
40
20
0
mitoplasts
POMP39
SAM35
POMP10
POMP25
POMP16
POMP9
POMP14
POMP40
B
-prot K
+prot K
POMP39
c-MYC
MCP-5
SAM35
HA
POMP10
POMP25
POMP16
POMP9
POMP14
POMP40

Figure 4

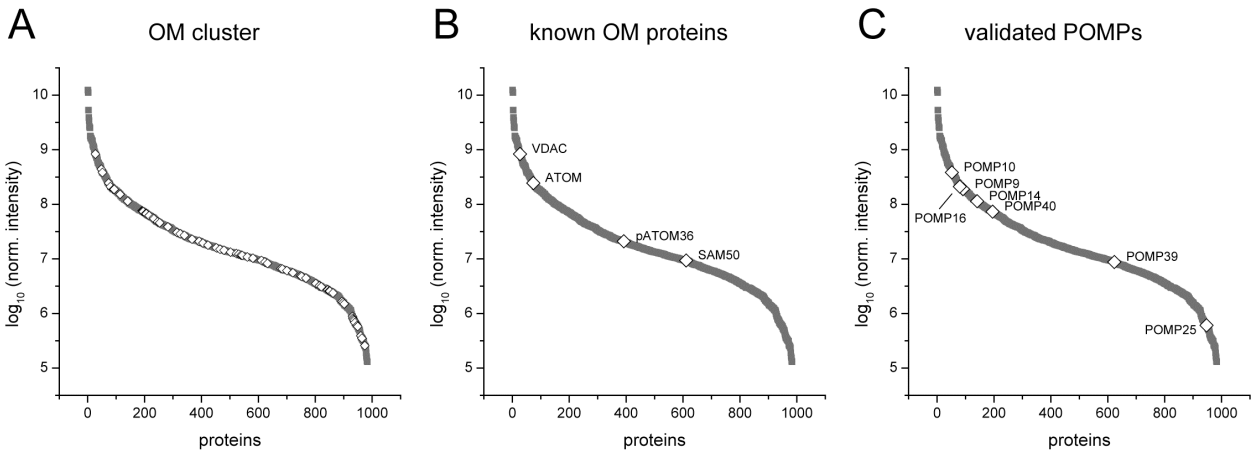
A
OM cluster
B
known OM proteins
C
validated POMPs
log10 (norm. intensity)
proteins
VDAC
ATOM
pATOM36
SAM50
POMP10
POMP9
POMP14
POMP40
POMP16
POMP39
POMP25

Figure 5

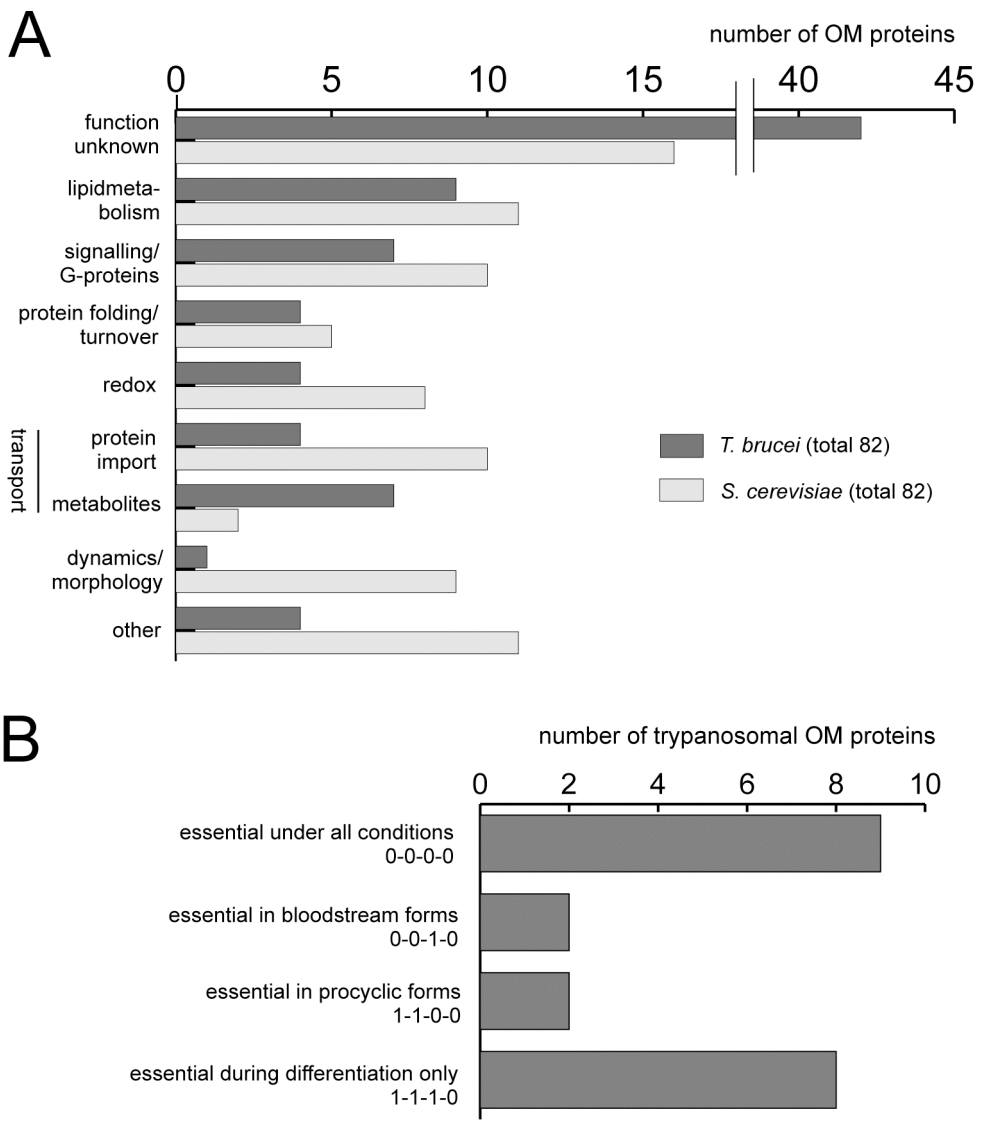
A
number of OM proteins
0
5
10
15
40
45
function unknown
lipidmeta-bolism
signalling/ G-proteins
protein folding/ turnover
redox
transport
protein import
metabolites
dynamics/ morphology
other
T. brucei (total 82)
S. cerevisiae (total 82)
B
number of trypanosomal OM proteins
0
2
4
6
8
10
essential under all conditions 0-0-0-0
essential in bloodstream forms 0-0-1-0
essential in procyclic forms 1-1-0-0
essential during differentiation only 1-1-1-0

Figure 6

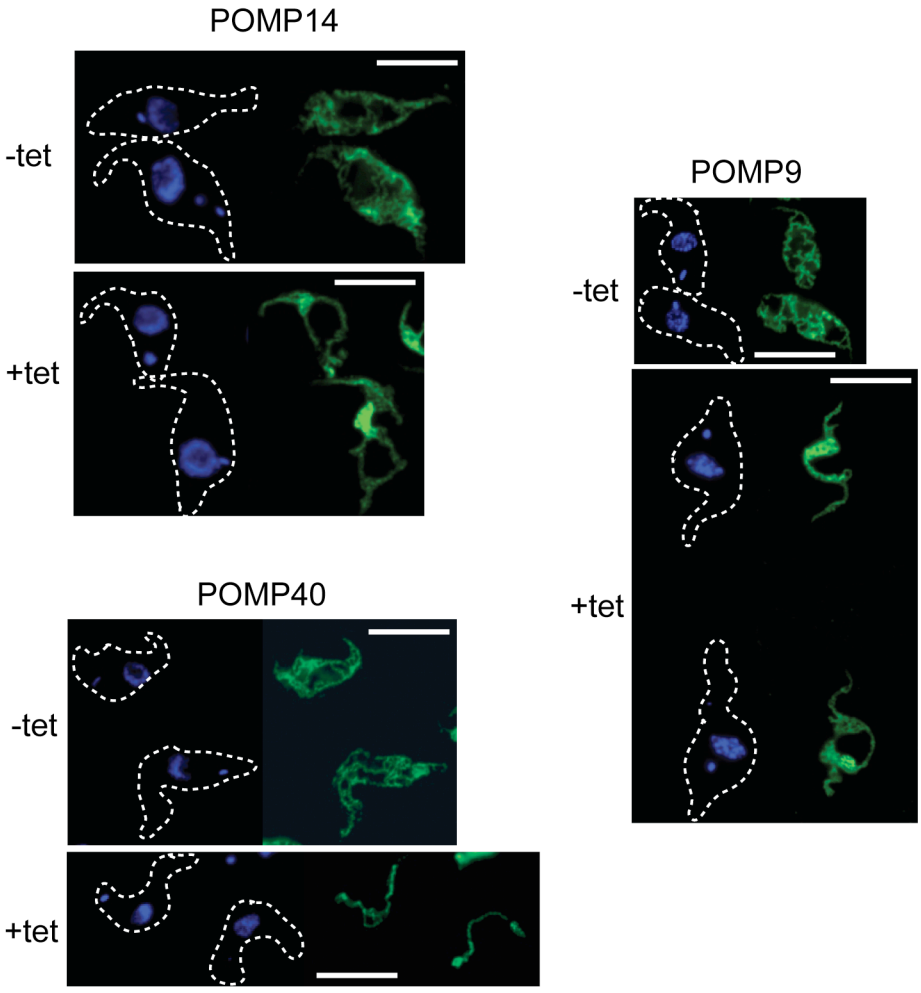

Figure 7